AN ABSTRACT OF THE THESIS OF

Kenneth James Sternes for the Master of Science in Department of Electrical and Electronics Engineering presented on April 3, 1967

Title: Impedance Bridge Balancing Using Perturbation Theory

Abstract approved: Redacted for Privacy

James C. Looney

This paper describes a technique for separating the two signal voltages which are necessary for balancing an ac impedance bridge from its detector output voltage. The technique is unique in that the necessary information is derived from modulations on the generator voltage. These modulations are formed by perturbing the variable arms at a fixed frequency but phased 90° apart. The two signals are then separated by phase detectors referenced to the modulation frequency and the proper phase. The perturbation increases and decreases the arm by a small amount; comparable to the action of a human operator increasing and decreasing the variable arm slightly to see which direction appears to lead to a null. Although no attempt was made to automate a bridge, this paper discusses the theoretical considerations for deriving the proper control signals for automating a bridge as well as experimental results obtained from a working model of such a system.

IMPEDANCE BRIDGE BALANCING USING PERTURBATION THEORY

by

KENNETH JAMES STERNES

A THESIS

submitted to

OREGON STATE UNIVERSITY

in partial fulfillment of
the requirements for the
degree of

Master of Science

June 1967

APPROVED:

Redacted for Privacy

Associate Professor of Electrical and Electronics Engineering

in charge of major

Redacted for Privacy

Head of Department of Electrical and Electronics Engineering

Redacted for Privacy

Dean of Graduate School

Date thesis is presented April 3, 1967

Typed by Erma McClanathan for Kenneth J. Stone

TABLE OF CONTENTS

I.	Introduction	1
II.	Perturbation Theory	8
III.	Experimental Results	21
IV.	Summary and Conclusions	28
	Bibliography	30
	Appendix A	31
	Appendix B	34

LIST OF FIGURES

Figure

1.1 Capacitance Bridge..... 2
1.2 Phase Plot of Tuned Detector..... 5
2.1 Perturbed Resistance Bridge..... 9
2.2 Bridge Output Case (I)..... 9
2.3 Rectified Output Case (I)..... 9
2.4 Bridge Output Case (II)..... 10
2.5 Rectified Output Case (II)..... 10
2.6 Bridge Output Case (III)..... 10
2.7 Rectified Output Case (III)..... 10
2.8 Half Bridge With Perturbing Elements..... 12
2.9 Loci of Bridge Output Voltage..... 12
2.10 Locus of Perturbed Bridge Output Voltage.... 14
2.11 Detector Output With Balance at C_1..... 14
2.12 Detector Output With Balance at C_2..... 17
2.13 Detector Output With Balance at C..... 18
2.14 Loci of Bridge Output for Small Deviations Around Balance..... 19
2.15 Locus of Bridge Output for Small Perturbation Near Balance..... 19
2.16 One-Dimensional Output Plot..... 19
3.1 Capacitance Bridge With Perturbing Elements. 22
3.2 Generator for Driving Perturbing Elements... 22
3.3 Multivibrator and Flip-Flop Waveforms..... 23
3.4 Demodulator Diagram..... 24
3.5 Perturbation System Block Diagram..... 25
A-1 Half of Capacitance Bridge..... 31
B-1 Capacitance Bridge With $R_D = R_X = q = 0$..... 34
B-2 Capacitance Bridge With $X_S = X_X = p = 0$..... 34
B-3 Perturbed Capacitance Bridge..... 37

LIST OF TABLES

Table

2.1 Switch Sequence Table..... 15

3.1 Empirical and Theoretical Values of R_D and R_V for Various Perturbation Magnitudes and Unknown Capacitors..... 27

B-1 Switch Sequence..... 37

IMPEDANCE BRIDGE BALANCING USING PERTURBATION THEORY

I. INTRODUCTION

AC impedance bridges are variable in two parameters that are proportional to the real and imaginary components or to the magnitude and phase of the unknown impedance. These bridges are balanced by adjusting two arms, and the adjustment after balance provides information about the unknown impedance.

To better understand the problems of automating ac impedance bridges, consider the procedure used by a human operator to balance one. The circuit shown in Fig. 1.1 is one of the more common capacitance bridges and will serve to illustrate the procedure. The two variable quantities in this bridge are R_V and R_D, where C_X is proportional to R_V, and the dissipation factor of C_X is proportional to R_D. To begin, R_V is adjusted for a minimum indication on the null detector; this will not be a true null since R_D is presumably not at its correct setting. Next R_D is adjusted to obtain a better balance. R_V can now be adjusted nearer to its balance point, and R_D may then be adjusted more precisely. Alternate adjustment of R_V and R_D will result in a null as precise as the capacitance measuring system is capable of resolving.

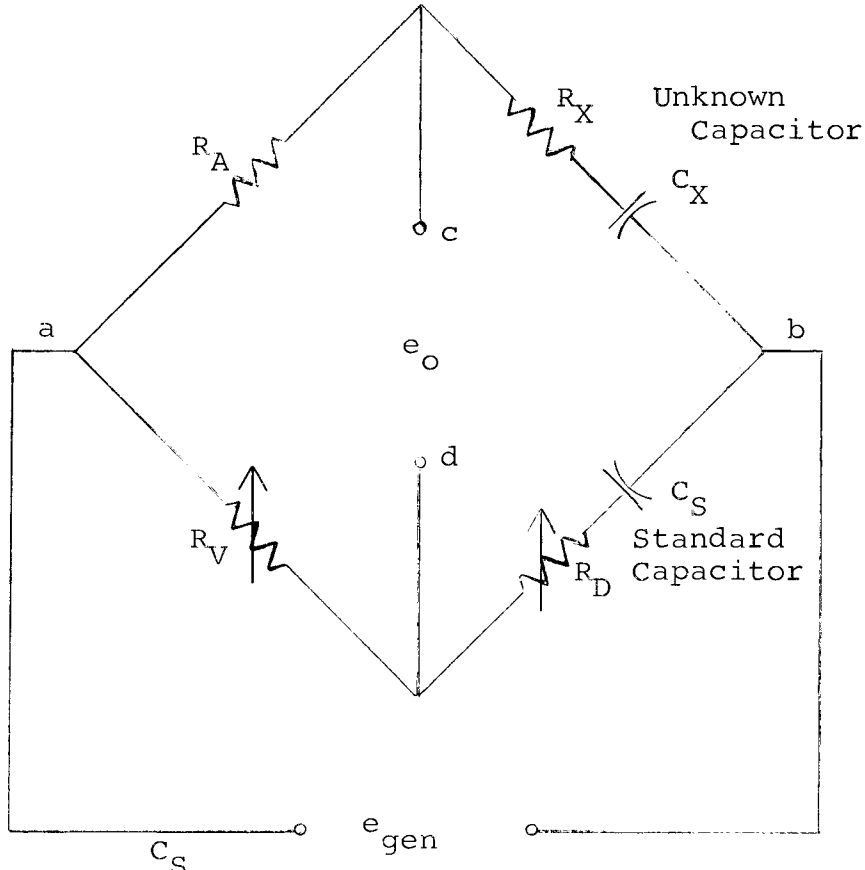

Figure 1.1. Capacitance Bridge.

To manually balance an ac impedance bridge, the operator must determine whether the variable arms need to be increased or decreased by trying one direction or the other and noting whether it increases or decreases the null detector reading. The operator must also learn to adjust both variable arms with the information provided by only one error signal, the detector voltage.

The principal difficulty in automating the balance of ac bridges is separating the output signal of the unbalanced bridge into two signals that will provide sufficient information to bring it to balance (7, p. 205-209). To date, the most practical method of separating the signals has been the use of phase-sensitive detectors (1, p. 110-116), but this method can practically be employed only if there is a constant phase relationship between the two control signals and some reference signal such as the bridge generator voltage. This is the case for some impedance bridges, but not the one shown in Fig. 1.1.

A second source of difficulty with phase-sensitive detectors is maintaining the proper phase relationships. To resolve to the accuracy often desired of a bridge, a sharply tuned detector is used to increase the signal-to-noise ratio. Unfortunately, this also implies a sharp phase shift at the resonant frequency. A phase

plot for such a detector using a twin-T network in a feedback path is illustrated in Fig. 1.2.

It is readily apparent from Fig. 1.2 that a slight shift in frequency of the bridge generator will result in a substantial change in the phase relationship between the generator and detector output.

McGrath and Rideout, in an article published by the IRE Professional Group on Automatic Control (5, p. 35-42), describe a perturbation scheme whereby they perturb the parameters of interest by a small amount, at a frequency much lower than that of the driving voltage. What they describe is a control system whereby sinusoidal perturbations of different frequencies are used and the signals separated with tuned amplifiers. It would appear, however, that one might consider an ac bridge in this same manner.

McGrath and Rideout also point out that square-wave perturbation rather than sine-wave would work equally well, as would two different phases rather than different frequencies. Since square-wave perturbations may be obtained easier than sine-wave and different phases easier to obtain than different frequencies, these innovations will be of considerable interest. For instance, the perturbations may be established by use of magnetic reed switches switching a small resistance or

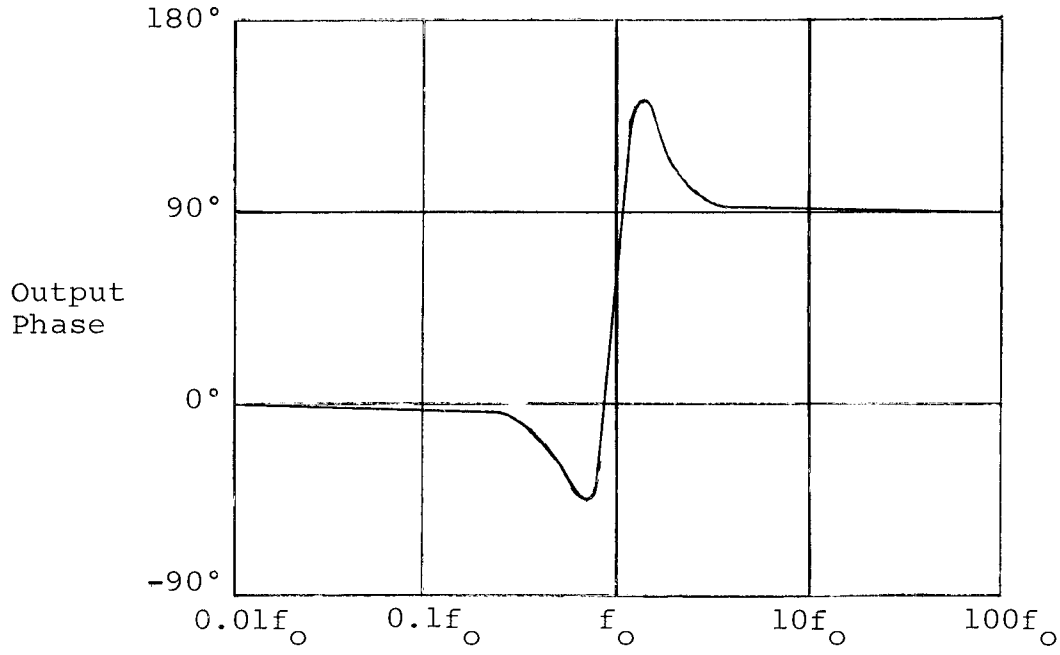

Figure 1.2. Phase Plot of Tuned Detector.

capacitance in or out of the respective arms of an impedance bridge.

In this case the signal, whose phase is of interest, is no longer at the frequency of the bridge generator but at the frequency of the perturbator, which may be only 0.01 of the bridge generator frequency. Looking again at the phase plot for a tuned detector, it can be seen that at such a frequency the output phase is virtually independent of frequency.

Thus, a tuned detector can be used without the danger of losing the necessary phase information due to a slight shift in the signal frequency. It is only necessary to restrict the Q of the tuned amplifier so that the sum or difference frequencies of the bridge generator and perturbation signal will be passed without severe attenuation. With perturbation frequencies on the order of 0.01 of the generator frequency, this will not be much of a restriction.

This paper will outline a technique using perturbation methods that will produce a control signal for each of the variable arms. It will be shown that these control signals will provide sufficient information to drive their respective variable arms to balance. A working model of such a bridge was built and is discussed. No attempt was made to actually automate the bridge, but

the necessary signals for driving a servo system or digital balancing system have been derived and demonstrated.

II. PERTURBATION THEORY

To see how the perturbation approach might be used with an ac bridge, consider the case of a simple ac resistance bridge (see Fig. 2.1). The generator frequency is much higher than the perturbation frequency. The output will be the generator frequency modulated by a square wave at the perturbation frequency, as can be seen from the equations for the output voltage:

$$e_o = \frac{R_a}{R_a + R_b} - \frac{R_c}{R_c + R_d} \Bigg|_{0}^{\frac{T}{2}} E_g \sin\omega t$$

$$e_o = \frac{R_a}{R_a + R_b} - \frac{R_c}{R_c + R_d + p} \Bigg|_{\frac{T}{2}}^{T} E_g \sin\omega t$$

where T is the period of the perturbation signal, ω the frequency of the generator voltage, and E_g the peak generator voltage.

There are three cases of interest: (I) $\frac{R_a}{R_a + R_b}$ larger than $\frac{R_c}{R_c + R_d}$, (II) $\frac{R_a}{R_a + R_b}$ smaller than $\frac{R_c}{R_c + R_d + p}$ and (III) $\frac{R_a}{R_a + R_b}$ equal to the average of $\frac{R_c}{R_c + R_d}$ and $\frac{R_c}{R_c + R_d + p}$. The output for each of these cases will appear as shown in Figs. 2.2 through 2.7.

If the dc component is removed from these outputs, the result is a square wave that goes through null and then reverses phase. Thus, by use of a phase-sensitive

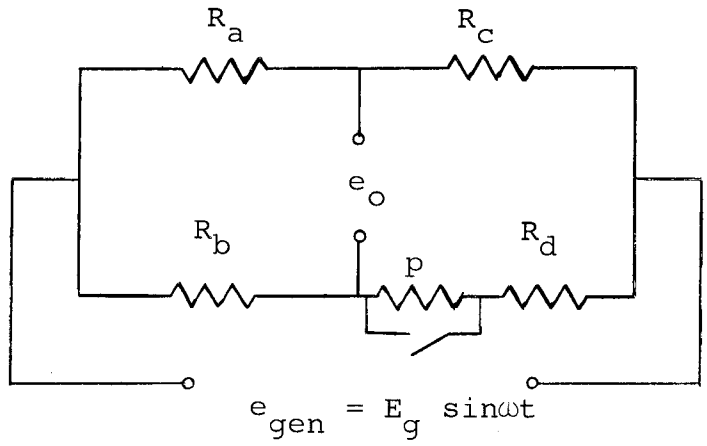

Figure 2.1. Perturbed Resistance Bridge.

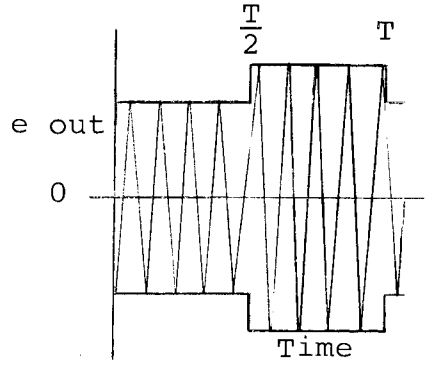

Figure 2.2. Bridge Output Case (I).

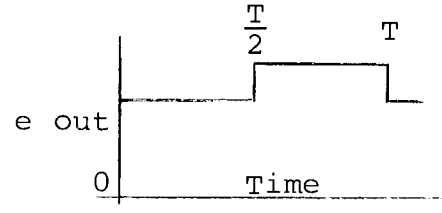

Figure 2.3. Rectified Output Case (I).

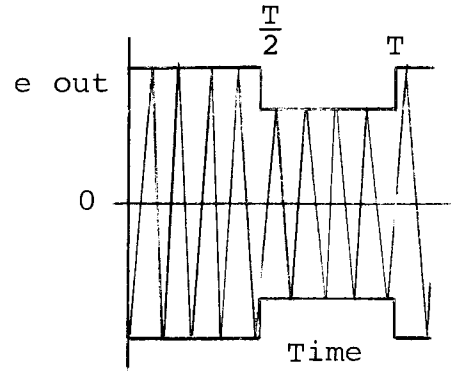

Figure 2.4. Bridge Output Case (II).

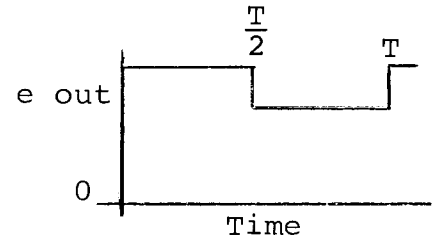

Figure 2.5. Rectified Output Case (II).

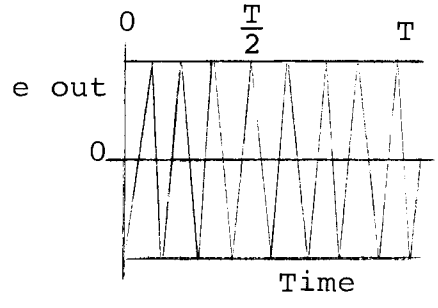

Figure 2.6. Bridge Output Case (III).

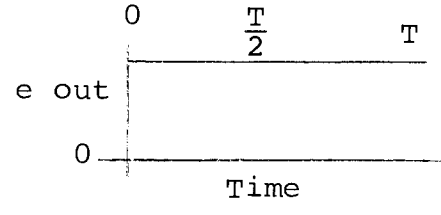

Figure 2.7. Rectified Output Case (III).

detector referenced to the perturbation generator, the necessary information for balancing the bridge can be obtained.

To show that this method works for a bridge variable in two parameters, consider again the capacitance bridge shown in Fig. 1.1, in particular, the half bridge containing the variable arms with the addition of perturbing elements as shown in Fig. 2.8.

Balance of the bridge occurs when the voltage e_{ad} equals the corresponding voltage of the other half of the bridge e_{ac}. Vector AB in Fig. 2.9 represents the voltage e_{ab}. Assume the generator impedance is low enough that its output is not affected by changes of settings of R_V and R_D. If R_D is held constant while R_V is varied, the locus of points at the tip of the vector that represents e_{ad} is a circle with its center on the perpendicular bisector of AB. Similarly, if R_V is held constant and R_D is varied, the locus is a circle that has its center on the Y axis. As can be seen in Fig. 2.9, these loci form families of circles. Appendix A gives the derivation of these loci.

If the perturbation switches, S_1 and S_2, are driven at the same frequency but with a 90° phase shift between them a pair of phase-sensitive detectors can be used to separate the two output signals. Each detector will be

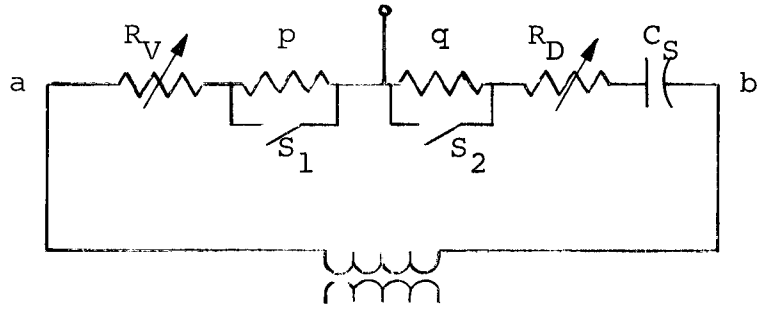

Figure 2.8. Half Bridge with Perturbing Elements.

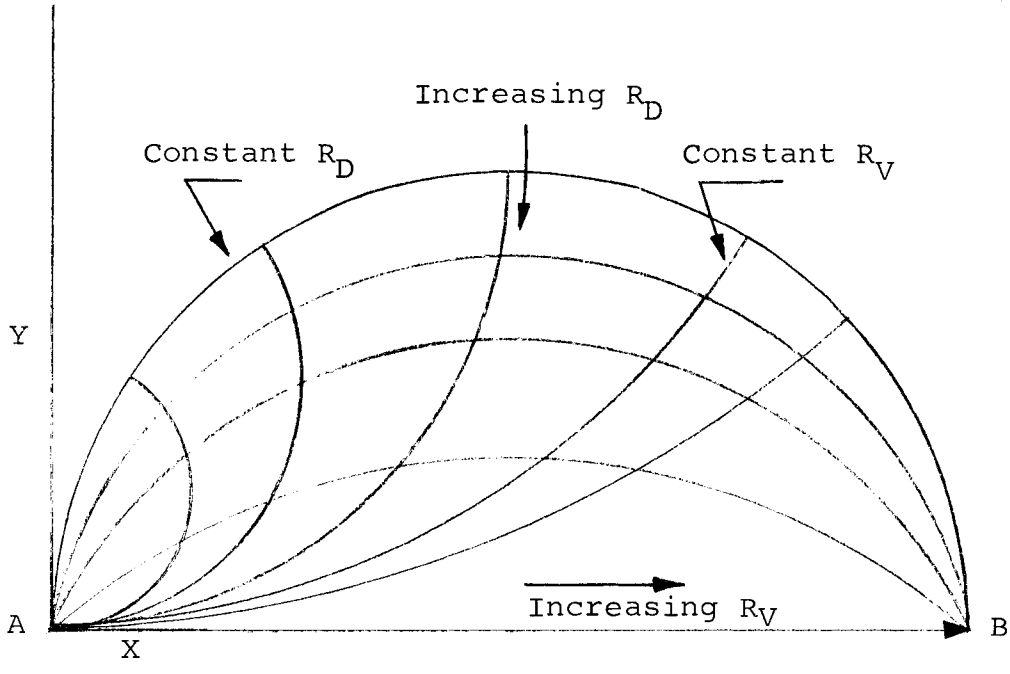

Figure 2.9. Loci of Bridge Output Voltage.

referenced to the phase of one of the switches. Since the two signals are 90° apart, the interaction of the two detectors will be at a minimum. A perturbation cycle that results in a 90° phase difference between switches is: both switches closed for one fourth the period of the cycle, one open (S_1) one closed (S_2) for the second quarter period, both closed for the third quarter, and one closed (S_1) the other open (S_2) for the last quarter.

In Fig. 2.10, point D represents the voltage e_{ad} with both perturbing elements shorted. D_1 represents voltage e_{ad} with switch S_1 open and S_2 closed, D_2 represents e_{ad} with S_1 and S_2 open, and D_3 represents e_{ad} with S_1 closed and S_2 open. Assume that C_1 represents the corresponding voltage of the other half of the bridge (i.e., e_{ac} in Fig. 1.1). The voltage at the input of the detector is the vector difference of these two vectors. The magnitude of the detector voltage is the distance from C_1 to D, D_1, D_2, or D_3, depending on the point in the perturbation cycle at which it is sampled. A plot of this envelope can be made corresponding to a plot of the detector output after rectifying and filtering. A plot for the point C_1 is shown in Fig. 2.11.

To better see what information is contained in this

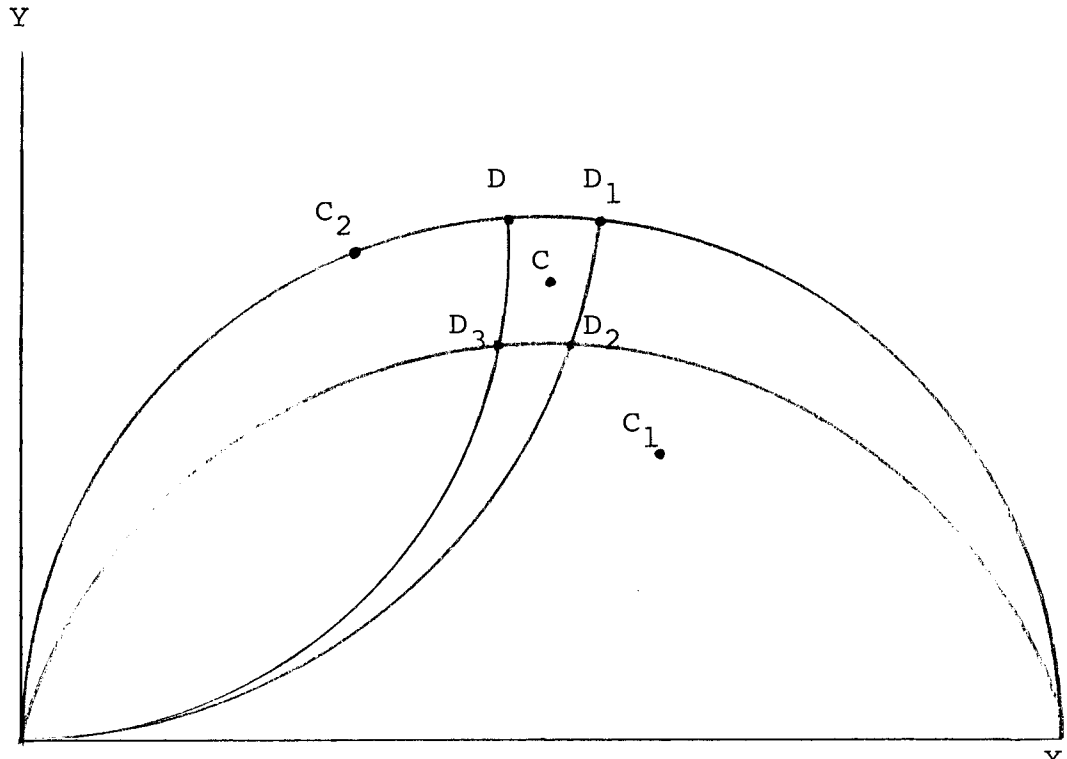

Figure 2.10. Locus of Perturbed Bridge Output Voltage.

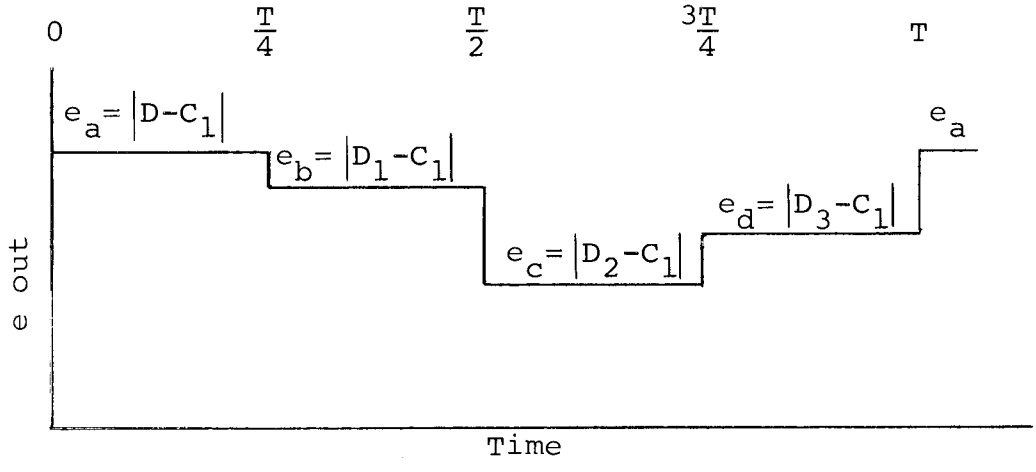

Figure 2.11. Detector Output With Balance at C_1.

waveform, consider it one section at a time with regard to what the perturbation switches are doing. This can be seen with the aid of Table 2.1. The output desired is proportional to the difference between the output with the switch of interest open and the output with the switch closed. The output which determines the positioning of R_V is the output at time a plus that at time c (S_1 closed) minus that at times b and d (S_1 open). The output for determining the position of R_D is the output at time a plus that at time b (S_2 closed) minus that at times c and d (S_2 open).

		Time			
		a	b	c	d
Switch	S_1	closed	open	open	closed
	S_2	closed	closed	open	open
		$e_a=D-C$	$e_b=D_1-C$	$e_c=D_2-C$	$e_d=D_3-C$
		Output			

Table 2.1. Switch Sequence Table

This formulation minimizes the influence of switch S_1 on the output that controls R_D. This can be seen by use of Table 2.1 and the equation for the output used to control R_D, $e_a+e_b-e_c-e_d$. It has the effect of summing the output of S_1 to 0 since it is a closed condition

minus a closed condition plus and open condition minus an open condition. Similarly the equation for the output used to control R_V is $e_{\underline{a}}-e_{\underline{b}}-e_{\underline{c}}+e_{\underline{d}}$ and results in a closed minus a closed plus an open minus an open condition as far as S_2 is concerned. Applying these equations to Fig. 2.11, it can be seen that the output for controlling R_D and R_V are both positive. Inspection of Fig. 2.10 shows that both parameters should be increased to obtain balance.

As another example, assume that C_2 is the output voltage for the other bridge half (e_{ac}). A plot for the detector envelope is shown in Fig. 2.12. The output for controlling R_D is negative as is the output for controlling R_V. Again by inspection of Fig. 2.10 this agrees with what is required, since in this case both parameters must be decreased to reach balance.

The final point of interest is C, which is located midway between D and D_2 and midway between D_1 and D_3. A plot of this envelope is shown in Fig. 2.13. Since $D-C=D_2-C$ and $D_1-C=D_3-C$ the outputs for control of R_V and R_D equals 0 indicating a balanced condition.

To show that this system gives the correct phase and balance information at or near balance with small perturbations, assume the arc segments are small enough to be considered straight lines. The loci of points

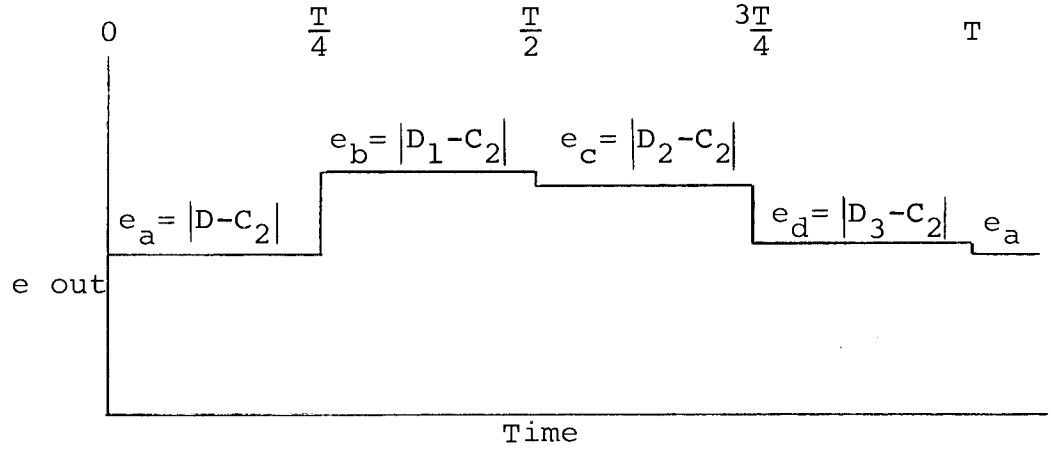

Figure 2.12. Detector Output With Balance at C_2.

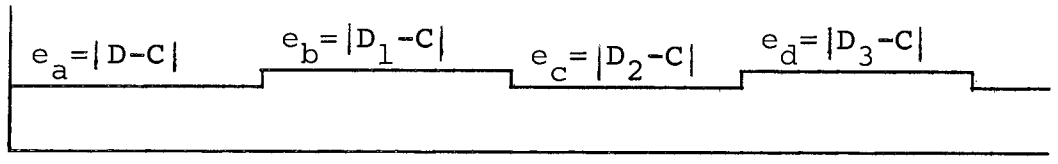

Figure 2.13. Detector Output With Balance at C.

representing the voltage e_{ad} while R_V is varied are a family of straight parallel lines. The loci of points obtained by varying R_D are also a family of straight parallel lines which intersect the lines described by varying R_V at some fixed angle. This forms a linear coordinate system as shown in Fig. 2.14.

The phase for controlling R_V is equal to the distance from p (an arbitrary point) to D_3 minus the distance of p to D_2 plus the distance p to D_1 minus the distance p to D. These lengths can be broken down into two components, one parallel to the constant R_D lines and the other perpendicular to them (see Fig. 2.15). Since the constant R_D lines are parallel, the perpendicular distances from two points on one of these lines to another constant R_D line will be equal. The only thing of interest in the difference between the two distances is the polarity so only the distances parallel to the constant R_D lines need be considered. A one-dimensional coordinate system can therefore be used to describe the outputs individually as shown in Fig. 2.16. It then becomes obvious that for p on the low side of the

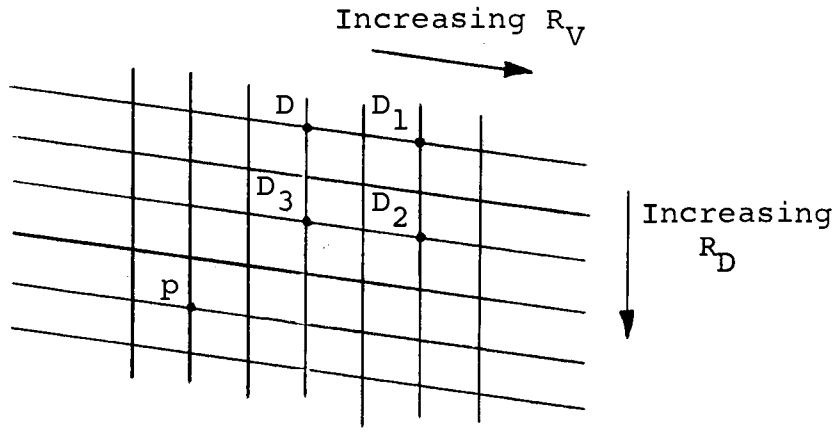

Figure 2.14. Loci of Bridge Output for Small Deviations Around Balance.

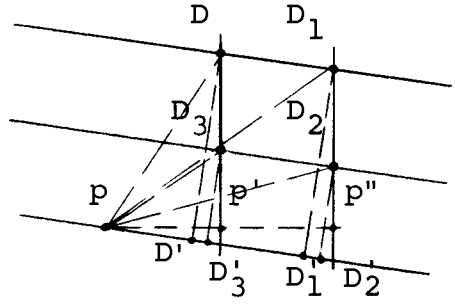

Figure 2.15. Locus of Bridge Output for Small Perturbation Near Balance.

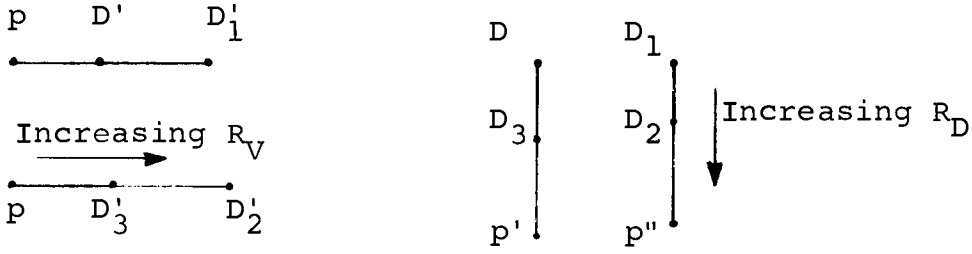

Figure 2.16. One-Dimensional Output Plot.

perturbation points, the difference of the two distances (i.e., $pD-pD_1$, pD_3-pD_2, $pD-pD_3$ and pD_1-pD_2) always taken in the same sequences, will be one polarity whereas if p is on the high side the differences will have the opposite polarity. Further, when p is equidistant between the two perturbation points, the difference will be 0. The path the parameters will take to reach balance will tend to follow the lines perpendicular to their constant value lines rather than follow the constant value lines of the other parameter. These lines intersect at the point described as the null point, however, so balance will still be achieved.

To show that the proper phase information is available no matter how far from balance the bridge is, consider the way the output could change phase. Except for going through the null point the only other way would be by traversing a path along the constant parameter lines that would separate the two points by more than 180°. This is impossible, however, within the limits of the described loci for this bridge. Thus it is seen here that the phase information will always be correct.

III. EXPERIMENTAL RESULTS

An experimental model was built using the concepts described. The basic bridge used was an ESI Model 290 Universal Impedance Bridge (see Fig. 3.1). It was used as a capacitance bridge, but the principle could be extended to inductance or ac resistance bridges.

The variable arms are R_V and R_D and are the parameters to be perturbed. The perturbation is accomplished by means of reed switches that switch small values of resistance in and out of the circuit.

In order to obtain the driving signal for the perturbating switches, an astable multivibrator was used to drive a pair of flip-flops as shown in Fig. 3.2. The output of the flip-flops is a pair of square waves with a 90° phase difference and half the repetition rate of the astable multivibrator (see Fig. 3.3).

Assume initially x y z are in the non-conducting, or up-state and $\bar{x}$ $\bar{y}$ $\bar{z}$ are in the conducting or down-state, then as x goes down and $\bar{x}$ up, flip-flop z will change state while y remains as before as shown in Fig. 3.3.

When X again changes state, flip-flop Y changes state while Z remains unchanged. The output of Y and Z may now be used to drive reed switches that will switch small impedances in and out of the bridge circuit.

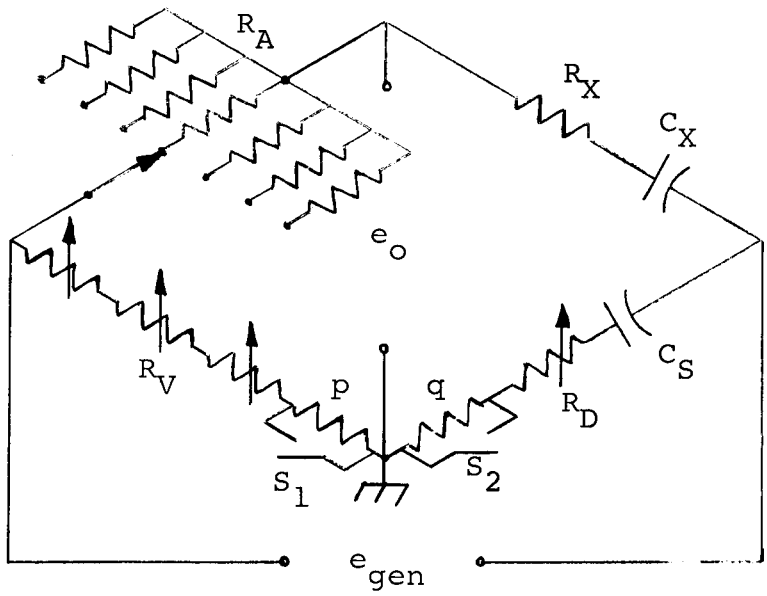

Figure 3.1. Capacitance Bridge With Perturbing Elements.

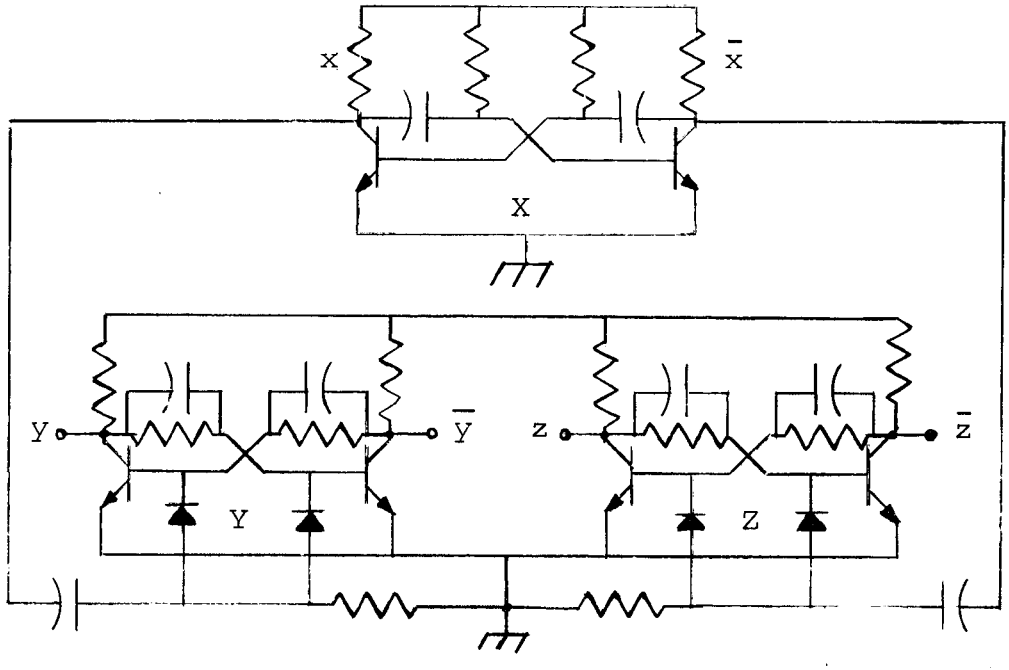

Figure 3.2. Generator for Driving Perturbation Switches.

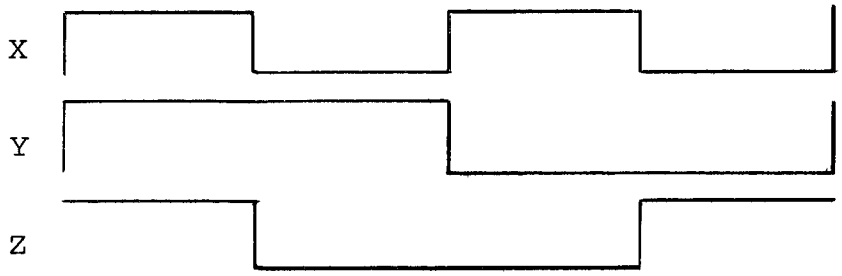

Figure 3.3. Multivibrator and Flip-Flop Waveforms.

The phase-sensitive detector for this system consists of a mechanical demodulator, four memory capacitors and buffer stages, and two summing amplifiers. The demodulator is driven from the same flip-flops that drive the perturbation switches. The circuit for this demodulator is shown in Fig. 3.4.

The four outputs, e_a, e_b, e_c, e_d, correspond to the four time intervals described in Table 2.1. The output at time interval a occurs when s_1 and s_2 are closed. This is equivalent to the logic statement Y and Z where Y is the flip-flop controlling s_1 and Z is the one controlling s_2. Similarly, the logic statements for the other three time intervals are b = $\bar{Y}$ and Z, c = $\bar{Y}$ and $\bar{Z}$, and d = X and $\bar{Z}$. These outputs from the summing amplifiers were then used to drive indicating meters, although they could have been used to drive a servo system to balance the bridge by varying R_D and R_V. A block diagram of this system is shown in Fig. 3.5.

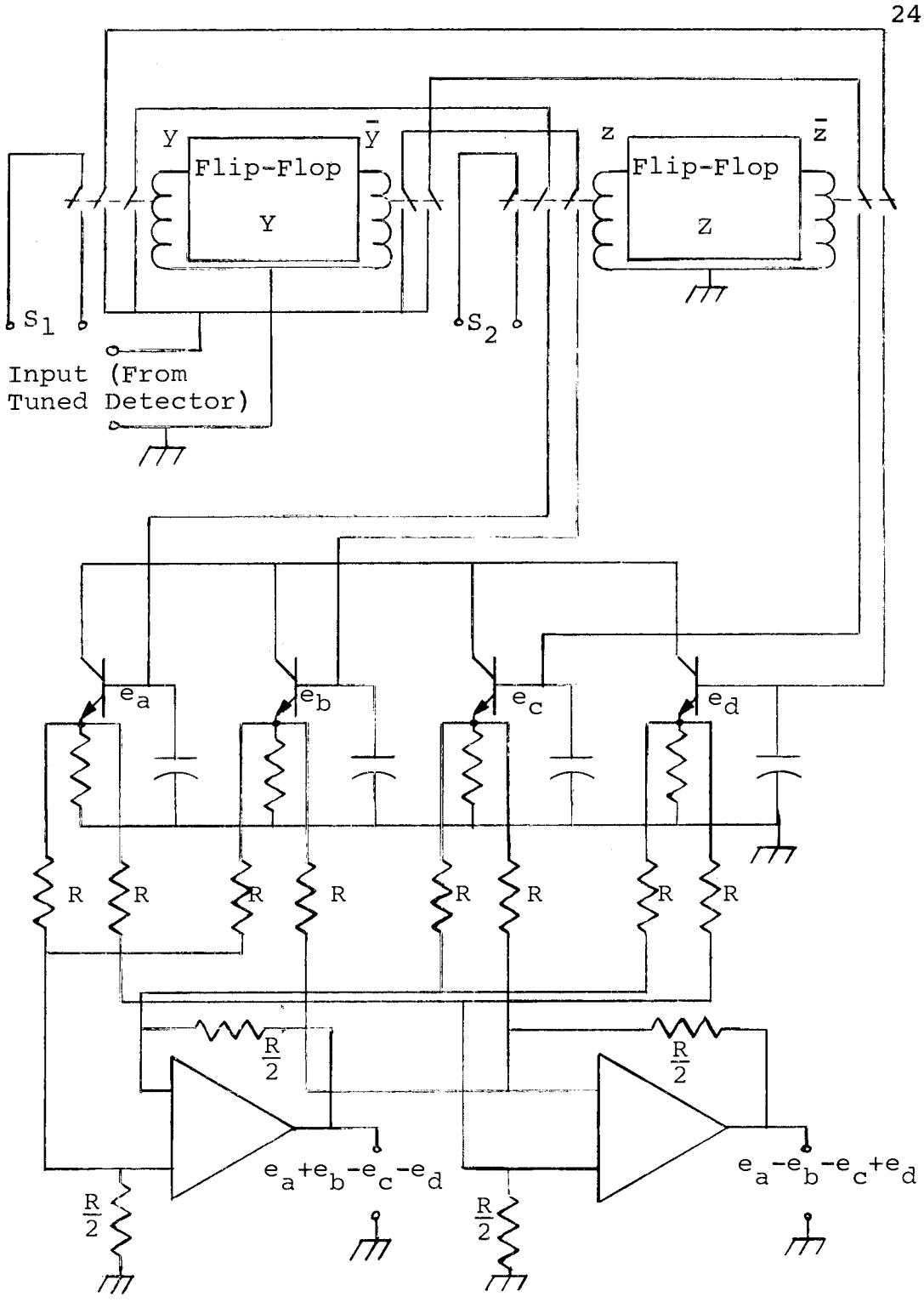

Figure 3.4. Demodulator Diagram.

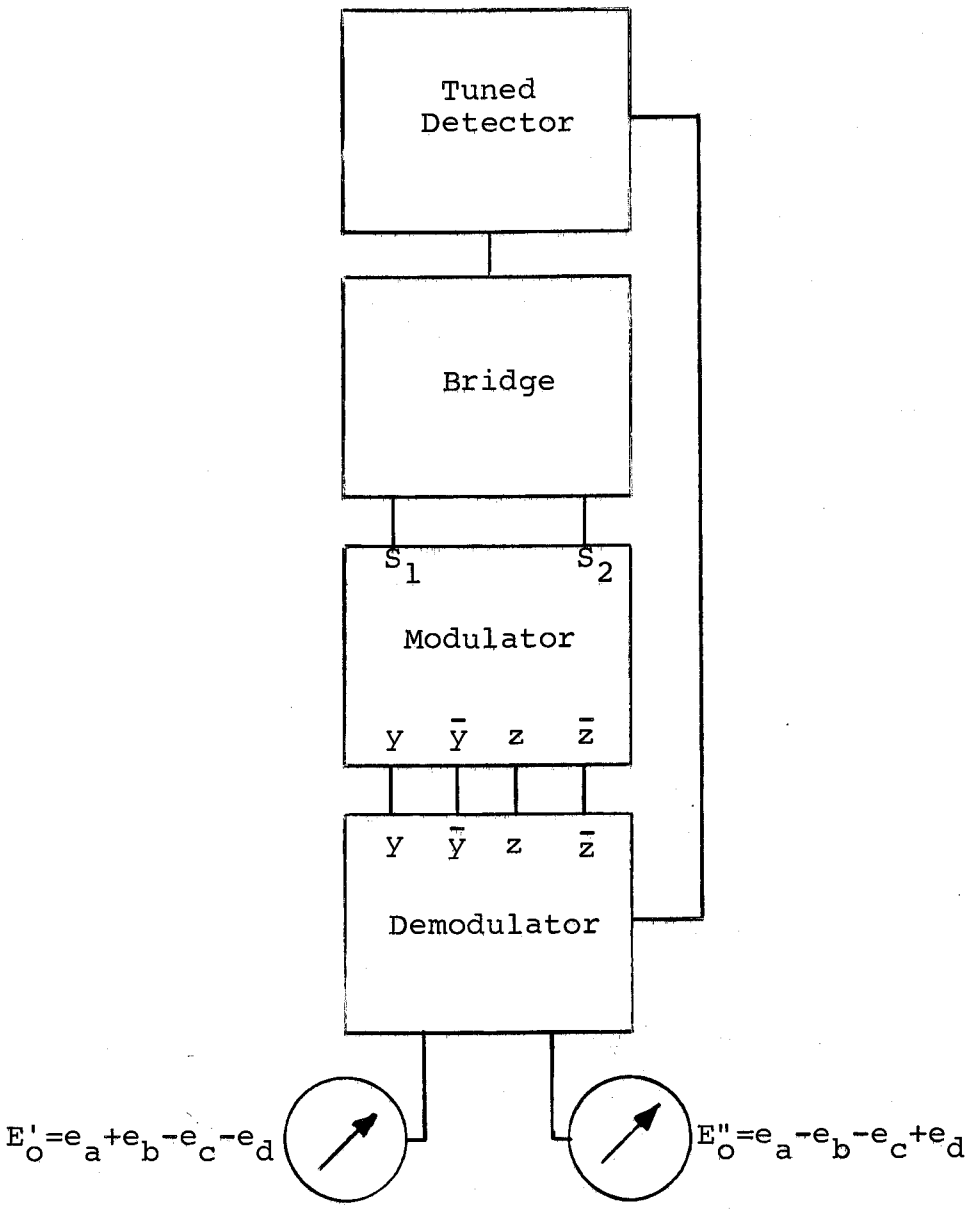

Where: E'_o is used to control R_D

E_o is used to control R_V

Figure 3.5. Perturbation System Block Diagram.

The balance equations for the bridge used are:

$$R_V = R_A \frac{C_X}{C_S} - \frac{p}{2} \qquad (1) \qquad R_D = R_X \frac{C_X}{C_S} - \frac{q}{2} \qquad (2)$$

These equations assume $p \ll R_V$ and $q \ll R_D$. For the derivation of these equations, see Appendix B.

The balance equations indicate R_V and R_D will be lower by half the magnitude of their perturbing elements at balance than they would be without the perturbations. Table 3.1 lists a group of measurements made with the bridge described together with the values for R_V and R_D calculated from the balance equations (1) and (2).

The measured values of R_D, even with perturbations as great as 20% of its magnitude, were as close to the calculated value as could be resolved on the bridge. The measured and calculated values for R_V likewise were within the resolution capabilities of the bridge. Perturbations exceeding 1% of R_V, however, required that the detector be attenuated so greatly that a sharp null could not be attained. Large perturbations were necessary with large unbalances, but did allow a closer null to be found. By decreasing the magnitude of the perturbation and increasing the detector sensitivity after an approximate null is found a sharper null can be attained. Starting from a random bridge setting, a null to the resolution capabilities of the bridge could be found

within four iterations of the above procedure.

Nominal Value of Unknown C	Perturbation Magnitude in Ohms		Bridge Balance in Ohms		Calculated Values in Ohms	
	p (R_V arm)	q (R_D arm)	R_V	R_D	R_V	R_D
1 nF	0	0	10011	49	10011	49
	1	0.16	10011	49	10011	49
	10	1.6	10006	48	10006	48
	100	16	9962	41	9961	41
100 nF	0	0	9995	15.2	9995	15.2
	1	0.16	9995	15.2	9995	15.1
	10	1.6	9990	14.3	9990	14.3
	100	16	9941	6.5	9945	7.2
10 μF	0	0	10016	9.2	10016	9.2
	1	0.16	10016	9.1	10016	9.1
	10	1.6	10011	8.0	10011	8.2
	100	16	9966	0.0	9966	1.2

Table 3.1. Empirical and Theoretical Values of R_D and R_V for Various Perturbation Magnitudes and Unknown Capacitors.

IV. SUMMARY AND CONCLUSIONS

It has been demonstrated that an ac impedance bridge can be automated using perturbation techniques. This technique has the advantage that it can be used with bridges for which there is no constant phase relation between the output signals and the generator. The phase information is contained in the perturbations, which are at a frequency far below the generator frequency. This allows a tuned detector to be used for a more precise balance without concern for losing phase information due to phase shifts within the tuned detector.

The principal disadvantage of this system is that with the capacitance bridge described, the two variable arms are dependent upon one another. For low loss capacitors, the degree of dependence is negligible and should have little or no effect on the balance procedure. As the dissipation factor increases, the bridge will still balance properly, but the balance time will be significantly increased.

The output voltage from most impedance bridges continuously decreases to a null as the bridge is balanced. The output voltage from the perturbation bridge, however, is nearly constant; assuming the amplitude of the perturbation is constant, until the variable arm is within

P/2 of balance, where P is the magnitude of the perturbation. Considering this fact, and that the magnitude of the perturbation and the gain of the detector must be varied in accordance with the degree of unbalance of the bridge, it would seem that a programmed digital balancing system would be better than a servo-balance system. Such a system could be programmed to begin each measurement with maximum perturbation magnitudes and detector attenuation, then with each successive refinement of the measurement, the amplitude of the perturbation and the detector attenuation can be reduced until the error introduced by the non-linearity of the perturbations is less than the accuracy of the bridge. The program could be to first complete one perturbation cycle, then compare the outputs of the phase sensitive detectors with a reference. If either or both outputs are above the reference level, their phase information could be used to adjust the variable arms to bring the bridge closer to balance. The perturbation cycle would then be repeated and the outputs of the phase-sensitive detectors checked. If both the outputs are below the reference level, the perturbation magnitude and detector attenuation would be reduced and the above process repeated until final balance is reached.

BIBLIOGRAPHY

1. Graham, J. F. Automatic A.C. bridges. Electronics 30:110-116. Feb. 1951.

2. Grinevich, F. B. Automatic bridges with external regulation and phase selection of controlling effects. Measurement Techniques 2:128-131. July 1962.

3. Grinevich, F. B. Design of automatic modulation A.C. bridges with an amplitude-phase detection. Measurement Techniques 11:944-948. June 1963.

4. Kneller, V. Iu. A.C. bridges with balancing in two parameters. Automation and Remote Control 19:156-166. Feb. 1958.

5. McGrath, R. J. and V. C. Rideout. A simulator study of a two parameter adaptive control system. Institute of Radio Engineers Transactions on Automatic Control AC-6:35-42. Feb. 1961.

6. McGrath, R. J., V. Rajaraman and V. C. Rideout. A parameter-perturbation adaptive control system. Institute of Radio Engineers Transactions on Automatic Control AC-6:154-162. May 1961.

7. White, W. E. The optimal conditions of convergence in A.C. bridge networks using phase selective indicators. Institute of Radio Engineers Transactions on Instrumentation I-6:205-209. Sept. 1957.

APPENDIX

APPENDIX A

Loci of Half Bridge Output

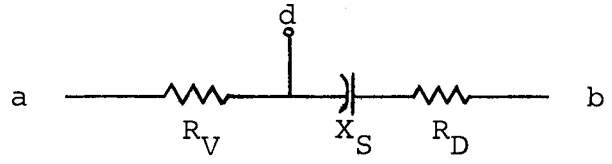

Figure A-1. Half of Capacitance Bridge.

If the voltage across ab is normalized to a unit vector with its tail at the origin and lying on the X axis, the X-Y coordinates of the tip of the vector, AD, representing the voltage across ad as R_V and R_D are varied, is found as follows:

$$e_{ab} = \frac{R_V}{R_V + R_D - jX_S} = x + jy \qquad (1)$$

$$\frac{R_V(R_V + R_D + jX_S)}{(R_V + R_D)^2 + X_S^2} = x + jy \qquad (2)$$

$$x = \frac{R_V\,(R_V + R_D)}{(R_V + R_D)^2 + X_S^2} \qquad (3)$$

$$y = \frac{R_V X_S}{(R_V + R_D)^2 + X_S^2} \qquad (4)$$

The locus of the tip of AD as R_V is varied while R_D is held constant can be determined by removing R_V from equations (3) and (4).

$$\frac{y}{x} = \frac{R_V X_S}{R_V(R_V + R_D)} = \frac{X_S}{R_V + R_D} \tag{5}$$

$$\frac{y}{x}R_V + \frac{y}{x}R_D = X_S \qquad \frac{y}{x}R_V = X_S - \frac{y}{x}R_D$$

$$R_V = \frac{x}{y}X_S - R_D \tag{6}$$

Substituting this value of R_V into equation (4)

$$y = \frac{(\frac{x}{y}X_S - R_D)X_S}{(\frac{x}{y}X_S - R_D + R_D)^2 + X_S^2} = \frac{(\frac{x}{y}X_S - R_D)X_S}{\frac{x^2}{y^2}X_S^2 + X_S^2}$$

$$\frac{x^2}{y}X_S^2 + yX_S^2 = \frac{x}{y}X_S^2 - R_D X_S$$

$$x^2 + y^2 - x + y\frac{R_D}{X_S} = 0$$

$$(x^2 - x + \tfrac{1}{4}) + (y^2 + y\frac{R_D}{X_S} + \tfrac{1}{4}\frac{R_D^2}{X_S 2}) = \tfrac{1}{4} + \tfrac{1}{4}\frac{R_D^2}{X_S 2}$$

$$(X - \tfrac{1}{2})^2 + (y + \tfrac{1}{2}\frac{R_D}{X_S})^2 = (\tfrac{1}{2})^2 + (\tfrac{1}{2}\frac{R_D}{X_S})^2 \tag{7}$$

Equation (7) describes a family of circles whose centers lie on the perpendicular bisector of the vector AB.

To determine the loci of the tip of AD with R_V held constant and R_D varied, remove R_D from equation (5).

$$R_D = \frac{x}{y}X_S - R_V \tag{8}$$

Substituting this value of R_D into equation (4)

$$y = \frac{R_V X_S}{(R_V + \frac{x}{y} X_S - R_V)^2 + X_S^2} = \frac{R_V}{\frac{x^2}{y^2} X_S + X_S}$$

$$\frac{x^2}{y} X_S + y X_S = R_V \qquad x^2 X_S + y^2 X_S - y R_V = 0$$

$$x^2 + (y^2 - y\frac{R_V}{X_S} + \frac{R_V^2}{4X_S^2}) = \frac{R_V^2}{4X_S^2}$$

$$x^2 + (y - \frac{R_V}{2X_S})^2 = (\frac{R_V}{2X_S})^2 \qquad (9)$$

Equation (9) describes a family of circles whose centers lie on the Y axis at the point $\frac{R_V}{2X_S}$.

APPENDIX B

Bridge Balance Point With Consideration Given Perturbation Magnitude

Consider first two special cases:

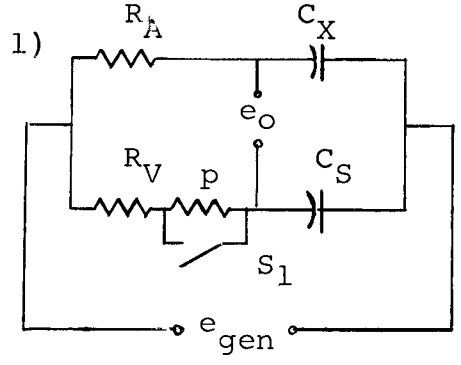

Capacitance Bridge With
$R_D = R_X = q = 0$

Figure B-1

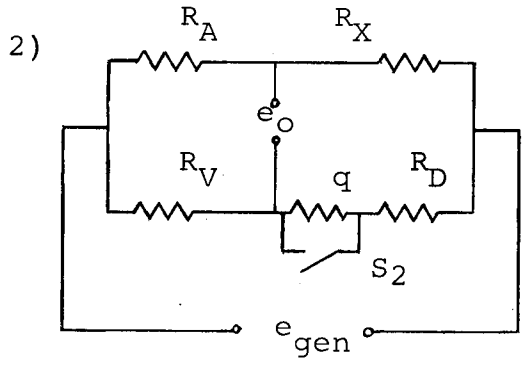

Capacitance Bridge With
$X_S = X_X = p = 0$

Figure B-2

Balance occurs when $e_o + e_o' = 0$. Where e_o is the output voltage with the perturbation switch closed and e_o' is the output voltage with it open.

For the first case the balance equations are:

$$\frac{-jX_X}{R_A-jX_X} - \frac{-jX_S}{R_V-jX_S} + \frac{-X_X}{R_A-jX_X} - \frac{-jX_S}{R_V-jX_S+p} = 0 \qquad (1)$$

Assume $\frac{p}{R_V-jX_s} << 1$ Then equation (1) simplifies to:

$$\frac{2X_X}{R_V-jX_X} - \frac{2X_S}{R_A-jX_S} + \frac{pX_S}{(R_A-jX_S)^2} = 0 \qquad (2)$$

Separating and equating the real and imaginary components of equation (2) to 0 yields:

$$2X_X R_V^2 - 2X_S R_A R_V + pX_S R_A = 0 \tag{3}$$

$$2R_V X_X - 2R_A X_S^2 + pX_S X_X = 0 \tag{4}$$

Solving equation (4) for R_V

$$R_V = R_A \frac{X_S}{X_X} - \frac{p}{2} \tag{5}$$

The balance equations for the second case are:

$$\frac{R_A}{R_A+R_X} - \frac{R_V}{R_V+R_D} + \frac{R_A}{R_A+R_X} - \frac{R_V}{R_V+R_D+q} = 0 \tag{6}$$

Assume $\frac{q}{R_V+R_D} << 1$

$$R_D^2 + R_D(R_V - \frac{R_V R_X}{R_A}) + (\frac{q}{2} + q\frac{R_X}{2R_A} - R_V\frac{R_X}{R_A})R_V = 0 \tag{7}$$

$$R_D = \frac{R_V(\frac{R_X}{R_A} - 1) \pm \sqrt{R_V^2(1+\frac{R_X}{R_A})^2 \quad (1-\frac{2qR_A}{R_A R_V + R_V R_X})}}{2}$$

$$R_D = R_V\frac{R_X}{R_A} - \frac{q}{2} \tag{8}$$

As can be seen from equations (5) and (8), the balance point occurs at a point lower by half the magnitude of the perturbing resistance than it would without the perturbation. This assumes only that the magnitude

of the perturbation is small compared to the variable arms.

To show that this solution holds for the general case, consider the balance equations for the complete bridge with no perturbations.

$$R_V = R_A \frac{X_S}{X_X} \qquad R_D = R_X \frac{X_S}{X_X}$$

Applying the above results to these balance equations produces the following equations which should be the balance equations for the perturbed bridge.

$$R_V = R_A \frac{X_S}{X_X} - \frac{p}{2} \quad (9) \qquad R_D = R_X \frac{X_S}{X_X} - \frac{q}{2} \quad (10)$$

This can be shown by substituting the values for R_V and R_D into the balance equations for the perturbed bridge. This consists of four equations, one for each time interval of the perturbation cycle. The absolute value of these equations can then be algebraically summed to represent the outputs of the two phase-sensitive detectors. The two expressions for the detector outputs are:

For control of R_D $e_o' = |G_a| + |G_b| - |G_c| - |G_d|$

For control of R_V $e_o'' = |G_a| - |G_b| - |G_c| + |G_d|$

where G_a, G_b, G_c, G_d are the transfer functions of the bridge at times a, b, c and d for the conditions shown in Table B-1.

		Time			
		a	b	c	d
Switch	S_1	Closed	Open	Open	Closed
	S_2	Closed	Closed	Open	Open

Table B-1. Switch Sequence.

The four equations corresponding to the time intervals of Table B-1 for the bridge shown in Figure B-3 are:

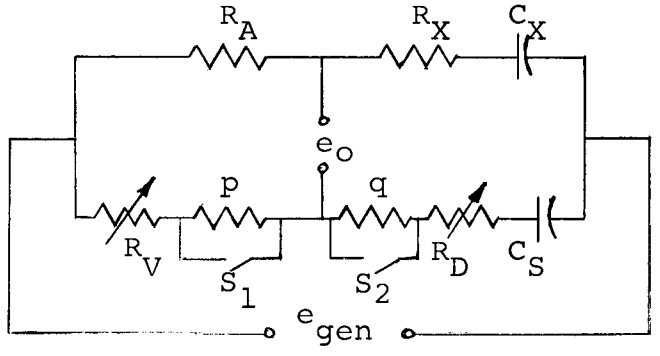

Figure B-3. Perturbed Capacitance Bridge

$$G_a = \frac{R_A}{Z_1} - \frac{R_V}{Z_2}$$

$$G_b = \frac{R_A}{Z_1} - \frac{R_V+p}{Z_2+p}$$

$$G_c = \frac{R_A}{Z_1} - \frac{R_V+p}{Z_2+p+q}$$

$$G_d = \frac{R_A}{Z_1} - \frac{R_V}{Z_2+q}$$

where:

$$Z_1 = R_A+R_X - \frac{j}{\omega C_X}$$

$$Z_2 = R_V+R_D - \frac{j}{\omega C_S}$$

Substituting the values found in equations (9) and (10) for R_V and R_D.

$$G_a = \frac{R_A}{Z_1} - \frac{R_A\frac{X_S}{X_X} - \frac{p}{2}}{Z_1(1-\frac{p+q}{2Z_1})\frac{X_S}{X_X}}$$

where:

$$X_X = \frac{1}{\omega C_X}$$

$$X_S = \frac{1}{\omega C_S}$$

Assuming $\frac{p+q}{2Z_1} << 1$

$$G_a = \frac{\frac{pX_S}{2X_X} - R_A\frac{p+q}{2Z_1}}{Z_1}$$

$$G_b = \frac{-\frac{pX_S}{2X_X} + R_A\frac{p-q}{2Z_1}}{Z_1}$$

$$G_c = \frac{-\frac{pX_S}{2X_X} + R_A\frac{p+q}{2Z_1}}{Z_1}$$

$$G_d = \frac{\frac{pX_S}{2X_X} - R_A\frac{p-q}{2Z_1}}{Z_1}$$

What is desired is the algebraic sum of the absolute value of the transfer functions. However, all that is needed is to determine whether or not they sum to zero. This can be determined by the algebraic sum of their squares.

$$G_a^2+G_b^2-G_c^2-G_d^2 = \frac{1}{4Z_1^2}\left[K^2-2KR_A\frac{p-q}{Z_1} + \left(R_A\frac{p+q}{Z_1}\right)^2-K^2+2KR_A\frac{p+q}{Z_1}\right.$$

$$\left.-\left(R_A\frac{p-q}{Z_1}\right)^2-K^2+2KR_A\frac{p+q}{Z_1}-\left(R_A\frac{p+q}{Z_1}\right)^2+K^2-2KR_A\frac{p-q}{Z_1}+\left(R_A\frac{p-q}{Z_1}\right)^2\right]=0$$

Where: $K = p\frac{X_S}{X_X}$

$$G_a^2-G_b^2-G_c^2+G_d^2 = \frac{1}{4Z_1^2}\left[K^2-2KR_A\frac{p+q}{Z_1}+\left(R_A\frac{p+q}{Z_1}\right)^2-K^2+2KR_A\frac{p+q}{Z_1}\right.$$

$$\left.-\left(R_A\frac{p-q}{Z_1}\right)^2-K^2+2KR_A\frac{p+q}{Z_1}-\left(R_A\frac{p+q}{Z_1}\right)^2+K^2-KR_A\frac{p-q}{Z_1}+\left(R_A\frac{p-q}{Z_1}\right)^2\right]=0$$

Thus it is shown that equations (9) and (10) are the balance equations for the perturbed bridge.